Assessment of quantitative zonal parameters of prostate gland in discrimination of normal, benign, and malignant conditions: are these the more reliable parameters in the diagnosis of prostate cancer?

L. KARACA[1], Z.M. ÖZDEMIR[1], A. KAHRAMAN[1], H. ÇELIK[2], S. KAYA[3]

[1]Department of Radiology, Medical Faculty, Inönü University, Malatya, Turkey
[2]Department of Urology, Medical Faculty, Inönü University, Malatya, Turkey
[3]Department of Radiology, Çam Sakura Hospital, Istanbul, Turkey

Abstract. – OBJECTIVE: Prostate cancer diagnosis and treatment are increasing in current public healthcare programs. An improved resolution multiparametric magnetic resonance imaging (MRI) has shown the potential to enhance the detection and differentiation of this medical condition. In this study, MR perfusion parameters were investigated in different ages and diseases to differentiate clinically significant prostate cancer.

PATIENTS AND METHODS: From January 2017 to December 2022, 72 consecutive patients, who had undergone multiparametric MR imaging were enrolled in this study. Four different patient groups were formed: (1) those with prostate cancer, (2) those with prostatitis, (3) those with benign prostate hyperplasia (BPH), and (4) a control group. Quantitative dynamic contrast-enhanced (DCE)-MRI pharmacokinetic parameters included K_{trans}, K_{ep}, V_e, and iAUG. Different measurements were obtained from both the peripheral and transitional zones (PZ and TZ, respectively). Means values were compared between groups based on a univariate analysis.

RESULTS: K_{trans} and K_{ep} values in the PZ were found to be statistically significantly lower in the control group ($p = 0.003$ and $p = 0.011$, respectively). It was seen that K_{trans} and V_e measurements obtained from PZ had a statistically significant determinant in detecting malignancy ($p = 0.013$ and $p = 0.036$, respectively). It was seen that K_{trans}, V_e, and iAUG obtained from the TZ showed a statistically significant difference in prostate cancer ($p = 0.025$, $p = 0.005$, and $p = 0.011$, respectively) in contrast to other cases. Peripheral V_e values were statistically significantly lower than those measured V_e values from the TZ in prostate cancer cases ($p = 0.002$) in contrast to the other cases.

CONCLUSIONS: Quantitative DCE-MRI parameters may vary according to age, disease, and zonal anatomy. These differences may contribute to the diagnosis of clinically relevant prostate cancer.

Introduction

Prostate cancer is the second most common cause of death in men after lung cancer[1]. As the elderly population increases, the incidence and treatment rate of clinically significant prostate cancer will also increase. Multiparametric magnetic resonance imaging (MRI) has led to improvements in the detection of clinically significant cancer. Dynamic contrast-enhanced (DCE) imaging is routinely used for prostate examinations[2-8]. Therefore, it is important to use quantitative evaluation for the DCE-MRI. Many studies[2,4,5,9-22] addressing the evaluation of prostate cancer with DCE-MRI are available[2,4,5,9-22]. However, overlaps in the separation of prostate cancer from normal prostate tissue can still be found.

DCE-MRI uses compartmental pharmacokinetic models of tracer kinetics to describe the microscopic processes that distribute contrast agent molecules between the vascular and extravascular spaces[23]. In the literature, significant differences were found in terms of K_{trans} and K_{ep} values in the peripheral zone (PZ) in cases of prostate cancer[22,24-26]. However, conflicting results for the transition zone (TZ) exist. Moreover, these differences are reported to vary depending on other prostate-related diseases, such as benign prostate hyperplasia (BPH) and prostatitis[5,27].

This study aimed to investigate the changes in DCE-MRI parameters according to age, zonal anatomy, and patient groups, thus revealing the benefits they will provide for the diagnosis of clinically significant prostate cancer.

Corresponding Author: L. Karaca, MD; e-mail: karacaleyla4@gmail.com;
                        leyla.karaca@inonu.edu.tr

Patients and Methods

Study Populations

Between 2017 and 2022, a total of 219 men underwent examinations for suspicion of prostate cancer because of elevated prostate-specific antigen (PSA) levels. Histopathological evaluations of 80 patients diagnosed with prostate cancer were screened. In this study, patients with prostate cancer and at least 85% of tumoral tissue in their prostate gland were included for histopathological examination. Sixteen of these patients had diffuse tumor tissue in all zones of the prostate as determined radiologically and pathologically (mean age 73.0 years, range 67.0-82.0). Nineteen patients (mean age 62.0, range 57.0-65.0) were diagnosed with benign prostate hyperplasia (BPH). Those patients were followed for at least two or more years. Nineteen patients (mean age 56.0, range 48.0-61.0) with biopsy-proven prostatitis were included in the study. Nineteen patients (mean age 34.5, range 27.0-56.0) without complaints were included in the study as the control group.

The final population included 72 patients in this study (Figure 1). Other patients with benign diagnoses were excluded from the study because they were not followed up for a satisfactory period of time. Some patients were excluded from the data analysis owing to substantial motion or artifacts during image acquisition on the MRI examination.

This retrospective institutional case-control study was approved by the Local Institutional Review Boards of Inonü University (No.: 2021/162). Written informed consent was obtained.

Image Analysis

MRI scans were reviewed with the Siemens Syngo *via* Workstation (Germany) by a genitourinary oncology specialist radiologist and senior radiologist. The readers were aware of the histopathological results. All patients were assessed on T2-weighted, diffusion-weighted imaging (DWI), and dynamic contrast-enhanced (DCE) T1-weighted images.

In all patients, the observer started with the analysis of the T2WI sequence. The observer analyzed each sequence of T2WI, DWI, and DCE-T1 WI separately. The reader radiologist segmented TZ and PZ on fusion DCE- T2 W images.

The data based on the average of eight different measurements taken from both the PZ and TZ were used (Figure 2). All regions of interest (ROI) were manually added to the images after consensus between the two radiologists.

Multiparametric MRI Protocol

All the scans were obtained with a 3 T Magnet (Siemens Healthcare, Force, Germany) using a body coil and 32-channel abdominal array. Axial T1WI and T2 W imaging were performed with a 3 mm slice thickness and a 1 mm gap. The imaging
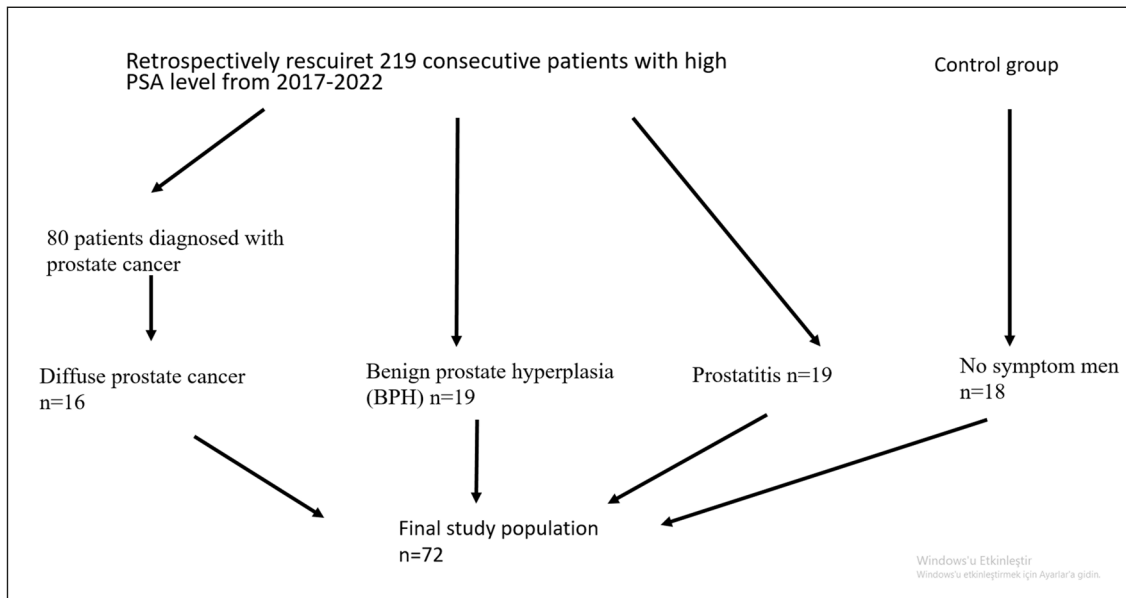

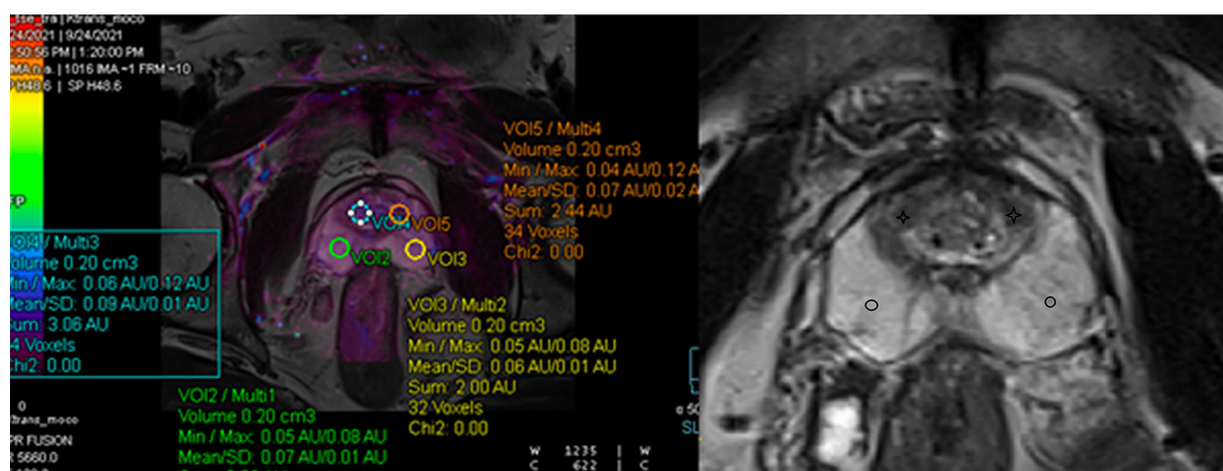**Figure 1.** The flowchart of study population.

Figure 2. Axial cross-section though the mid gland of a 45-year old man. Measurements of region of interest (ROI) values in the central (star) and peripheral zone (round) can be viewed.

field-of-view (FOV) was 14 cm, and the acquisition matrix was 256. The following MRI images were acquired in all patients: (1) axial, (2) sagittal, and (3) coronal turbo spin echo (TSE) T2WI, (4) axial conventional DWI, (5) axial Zoomit DWI, (6) DCE-MRI, and (7) T1WI after contrast injection. Gadodiamid (Omniscan, GE Health Care, USA) was injected into a peripheral vein prior to the MRI procedure. The DCE-MRI measurement was performed with VIBE (Volumetric Interpolated Breath-hold Examination-Siemens, Germany) imaging with a 24 cm FOV and matrix 256 x 192.

Statistical Analysis

Data analysis was performed using IBM SPSS Statistics version 25.0 software (IBM Corp., Armonk, NY, USA). To investigate whether the normal distribution and variance homogeneity assumptions were met, the Kolmogorov-Smirnov and Levene tests, respectively, were used. Categorical data were expressed as numbers (n) and percentages (%), while quantitative data were presented as mean ± standard deviation (SD) and median (25th-75th) percentiles. The mean differences among groups were evaluated using a one-way analysis of variance (ANOVA). When the p-values from the one-way ANOVA were statistically significant, a post-hoc Tukey HSD or Dunn-Bonferroni multiple comparison tests was used to understand which group differed from the others. The Wilcoxon Sign Rank test was applied for the comparisons of other radiological measurements (namely, K_{trans}, K_{ep}, V_e, and iAUG) between central and peripheral regions within each group. Categorical data were analyzed by Pearson's χ^2

test. Degrees of association between continuous variables were evaluated by Spearman's rank-order correlation analysis. The optimal radiological thresholds to determine malignancy were evaluated based on ROC analyses, which yielded the maximum sum of sensitivity and specificity for the significant test. The sensitivity, specificity, positive and negative predictive values, and accuracy levels for each significant radiological measurement were also obtained. Multivariate logistic regression analysis *via* a forward elimination was performed to determine the best predictors that discriminate study groups from each other. Any variable that was found to produce a statistically significant effect in the univariate analysis was accepted as a candidate for the multivariable model, along with all variables of known clinical importance. The odds ratios (OR), 95% confidence intervals (CI), and Wald statistics for each independent variable were also calculated. A p-value < 0.05 was considered statistically significant. However, for all possible multiple comparisons, the Bonferroni correction was applied for controlling Type I error.

Results

Patient Demographics and Clinical Features

The mean age of the patients with prostate cancer was 73.0 (67.0-82.0) years. The mean age of prostatitis patients was 56.0 (48.0-61.0) years. Nineteen patients were proven to have BPH histopathologically. The mean of these patients was 62.0

(57.0-65.0) years. These patients were followed for at least two or more than two years. Eighteen healthy volunteer patients without complaints were included in the study. The mean age of the patients was 34.5 (27.0-56.0) years. All groups showed significant differences in terms of age ($p < 0.001$).

Central and Peripheral Pharmacokinetic Parameters in Each Group

No statistically significant differences in K_{trans} and K_{ep} values in the central zone and PZ in young volunteers ($p > 0.05$) were found. Peripheral V_e values were significantly lower in comparison to central values ($p = 0.002$).

There was no statistically significant difference in V_e values between transition and peripheral zones in BPH group ($p > 0.05$). Peripheral K_{trans}, K_{ep}, and iAUC values were significantly lower in comparison to central values, respectively ($p = 0.003$, $p = 0.011$, and $p = 0.006$). The only value that showed a significant difference in the prostatitis group was K_{trans}. Peripheral K_{trans} was significantly lower in comparison to central values ($p = 0.007$) (Table I).

Significant differences were not observed based on the Bonferroni correction for the K_{ep} and V_e values in the prostate cancer group. K_{trans} and iAUG values were significantly low in the PZ in this group.

Comparison of Pharmacokinetic Parameters Between Patient Groups

All central values were found to be statistically similar between groups. In the comparison of groups, peripheral K_{trans}, iAUG, and V_e values were significantly higher in the prostate cancer patients than in the other groups ($p = 0.018$, $p = 0.009$, and $p = 0.017$, respectively). When the PZ of young volunteers and the BPH group were compared, K_{ep} values were found to be low in BPH ($p = 0.011$).

No statistically significant correlations between the centrally measured K_{trans}, K_{ep}, Ve, and iAUG measurements and age were found according to Bonferroni correction within the groups ($p > 0.00625$). In the PZ, BPH, Prostatitis, and Cancer groups, K_{trans}, K_{ep}, V_e, and iAUG values were not correlated with age.

In the young benign group, peripheral K_{trans} and V_e levels showed a significant decrease corresponding to age (r = -0.798 and $p < 0.001$ and r = -0.623 and $p = 0.006$, respectively).

The variables, their correlation coefficients, and significance levels are shown in Table II.

ROC Analyses

In the detection of both peripheral and central zones malignancy, it was seen that the iAUC, V_e, and K_{trans} values showed statistically significant differences. K_{ep} values were not statistically significant in terms of detecting malignancy (Figure 3).

Table I. Intra- and inter-group comparisons in terms of radiological measurements.

	Group 1	Group 2	Group 3	Group 4	*p*-value[†]
K_{trans}					
Central	0.16 (0.14 - 0.20)	0.18 (0.13 - 0.25)	0.16 (0.11 - 0.24)	0.21 (0.18 - 0.28)	0.142
Peripheric	0.12 (0.09 - 0.22)	0.10 (0.05 - 0.14)[a]	0.08 (0.06 - 0.18)	0.20 (0.13 - 0.23)[a]	**0.017**
p-value[‡]	0.647	**0.003**	**0.007**	**0.004**	
K_{ep}					
Central	0.55 (0.40 - 0.65)	0.57 (0.40 - 0.71)	0.58 (0.41 - 0.87)	0.53 (0.33 - 0.80)	0.904
Peripheric	0.56 (0.48 - 0.76)[b]	0.31 (0.19 - 0.50)[b]	0.42 (0.18 - 0.64)	0.48 (0.32 - 0.78)	0.014
p-value[‡]	0.145	**0.011**	0.014	0.605	
V_e					
Central	0.30 (0.26 - 0.44)	0.32 (0.26 - 0.44)	0.32 (0.22 - 0.41)	0.39 (0.37Ω - 0.55)	0.050
Peripheric	0.23 (0.19 - 0.30)[c]	0.32 (0.27 - 0.39)	0.30 (0.18z - 0.44)	0.35 (0.29z - 0.47)[c]	**0.023**
p-value[‡]	**0.002**	0.809	0.601	0.034	
iAUG					
Central	0.19 (0.17 - 0.27)	0.19 (0.14 - 0.28)	0.19 (0.14 - 0.28)	0.26 (0.22 - 0.33)	0.090
Peripheric	0.15 (0.11 - 0.24)	0.13 (0.06 - 0.16)[a]	0.11 (0.08 - 0.30)	0.23 (0.17 - 0.27)[a]	0.014
p-value[‡]	0.433	**0.006**	0.016	**0.004**	

Data were shown as median (25th-75th) percentiles. [†]The comparisons among groups, the Kruskal-Wallis test, according to the Bonferroni correction $p < 0.025$ was considered statistically significant. [‡]The comparisons between central and peripheric within each group, Wilcoxon sign rank test, according to the Bonferroni correction $p < 0.0125$ was considered statistically significant. [a]: Group 2 *vs.* Group 4 ($p < 0.025$), [b]: Group 1 *vs.* Group 2 ($p = 0.011$), [c]: Group 1 *vs.* Group 4 ($p = 0.017$).

Table II. The results of correlation analyses between age and radiological measurements within each group.

	Central		Peripheric	
	Coefficient of correlation	***p*-value†**	**Coefficient of correlation**	***p*-value†**
Group 1				
K_{trans}	-0.220	0.381	-0.798	<0.001
K_{ep}	0.117	0.645	-0.559	0.016
V_e	-0.510	0.031	-0.623	0.006
iAUG	-0.055	0.829	-0.471	0.049
Group 2				
K_{trans}	0.222	0.362	-0.063	0.797
K_{ep}	0.300	0.212	0.054	0.827
V_e	-0.244	0.315	0.197	0.419
iAUG	0.264	0.275	-0.022	0.929
Group 3				
K_{trans}	-0.200	0.413	-0.323	0.178
K_{ep}	0.009	0.972	-0.222	0.362
V_e	-0.178	0.465	-0.070	0.775
iAUG	-0.335	0.161	-0.535	0.018
Group 4				
K_{trans}	-0.099	0.716	0.164	0.545
K_{ep}	0.099	0.716	0.159	0.556
V_e	-0.231	0.389	-0.091	0.736
iAUG	-0.270	0.312	0.165	0.541

†Spearman's correlation analyses, according to the Bonferroni correction $p < 0.00625$ was considered statistically significant.

When the groups were compared, significant differences in prostate cancer groups in both the peripheral and central zones were found. Significant differences between the groups in terms of the distribution of central K_{trans}, V_e, and iAUC levels were noted. Significant differences between the groups in terms of the distribution of peripheral K_{trans}, V_e, and iAUC levels were detected. The cut-off point for the central K_{trans} in terms of distinguishing malignancies was 0.71, and the sensitivity of K_{trans} at this point was 93,8%, specificity 51.8%, positive and negative predictive values, 35.7% and 96.7%, respectively, and diagnostic accuracy 61.1%.

The sensitivity, specificity, and positive and negative predictive values of the central V_e value were 81.3%, 67.9%, 41.9%, and 92.7%, respectively. The cut-off and accuracy of the V_e value were 0.360 and 79.9%, respectively.

The cut-off point peripheral K_{trans} for distinguishing malignancies was 0.128. The sensitivity of K_{trans} at this point was 81.3%, specificity 62.5%, positive and negative predictive values 38.2% and 91.1%, respectively, and the diagnostic accuracy was 66.7%.

In addition, the most relevant central and peripheral measurements for distinguishing the study groups were determined using a multinomial logistic regression analysis. As a result of a forward stepwise logistic regression analysis, the most decisive factor in distinguishing groups from each other was V_e.

Discussion

DCE-MRI has been used frequently for the diagnosis of prostate cancer in recent years. However, points that need to be fine-tuned to increase clinical validity can be found. To our knowledge, this study is the first one to compare a normal group with cancer and other prostate pathologies. In the group of young males, central V_e values were found to be higher than peripheral values. Van Niekerk et al[28] reported that large variability was seen in central-transition zone-associated microvascular parameters. High central V_e values can be explained by hormonal changes and high microvascularity.
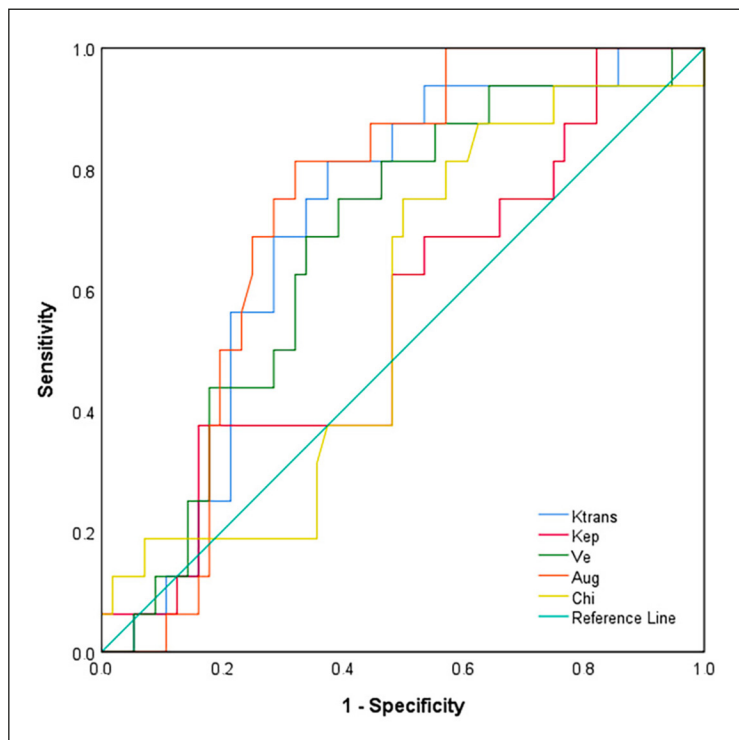
Figure 3. Receiver operating characteristic (ROC) curve shows sensitivity and specificity for all parameters in all groups.

K_{trans} and V_e levels measured from the peripheral zone decreased statistically with increasing age. Cannarella et al[29] reported that both age and hormones affect both prostate size and growth. We think that the decrease in the PZ could have been due to decreased blood vascularity or hormonal changes with age. In the literature, it has been shown that K_{trans} increases in prostate cancer[5,26,30]. This finding could explain why K_{trans} is first noticed in the PZ in prostate cancer cases.

In the BPH group, K_{trans}, K_{ep}, and iAUG were lower in the PZ compared to the TZ. Ma et al[31] reported that K_{trans}, K_{ep}, and V_e in prostate cancer were higher than in the BPH group. However, only obtained pharmacokinetic data was obtained by targeting the lesions, not the prostate zonal anatomy. This paper first gives brief pharmacokinetic parameters of BPH in the zonal anatomy. When the young and old benign groups were compared, the K_{ep} value in the PZ was found to have significantly decreased in the elderly group. Heverhagen et al[9] reported that five alpha-reductase inhibitors caused a reduction in the K_{ep} value in the PZ in dogs with induced BPH. This is similar to our findings, and it may explain why the K_{ep} value decreases in BPH patients.

In this study, it was found that K_{trans}, iAUG, and V_e values from each zone showed a statistically significant relevance when diagnosing malignancy. Similar studies[5,30,32-34] addressing the K_{trans} values are available in the literature. Most studies[5] found that K_{ep} values increased in the peripheral and central zones of prostate cancer cases. Our results were different in terms of K_{ep} values. We only found that K_{ep} values were significantly different in terms of the differential diagnosis of PZ prostate cancer. Gao et al[5] reported that consideration of K_{ep} values for differentiating prostate cancer from noncancerous central tissue is controversial. Abnormally increased K_{trans} and K_{ep} values in prostate cancer are thought to be associated with increased microvessel density and leaky vascular structures, which are reflections of tumoral neoangiogenesis.

A few studies[30,33] report that the V_e values are higher in prostate cancer than in noncancerous PZ zones. Cai et al[33] reported that the significant V_e values found in their study could be explained by the recruitment of a large number of patients with advanced prostate cancer. Our study described advanced prostate cancer in both PZ and TZ. We also found that peripheral and central V_e values were higher than in other groups. We can conclude that the increase in V_e value indicates high-grade prostate cancer, no matter where it is located. We can use the cut-off value of V_e to discriminate high-grade prostate cancer.

In our study, the V_e values in prostatitis and prostate cancer cases were significantly higher than in other groups. Uysal et al[27] reported that the V_e values were significantly higher in prostatitis lesions[27]. However, we did not find a significant difference in the value of Ve between prostate cancer and prostatitis cases. In this study, peripheral V_e values were statistically significantly lower than the V_e values measured in the TZ in prostate cancer cases. Although it has been reported to be controversial in the literature, we think this parameter may contribute to the diagnosis of clinically significant prostate cancer.

Limitations

Our study has several limitations. First, its retrospective design. Our patient population is relatively small. Larger samples are required to validate our study results. The other limitation of the study is the change in age and/or BPH can affect the transition and central zones. Another limitation is high grade of the patients in the cancer groups, which may affect the results.

Conclusions

Our results showed that V_e, K_{trans}, K_{ep}, iAUC significantly changed according to age, disease status, and zonal anatomy. We think that our findings may contribute to future studies. V_e, K_{trans}, and iAUC were found to strongly indicate malignancy, but zonal anatomy also affects these values. In our opinion, in the evaluation of clinically significant prostate cancer, understanding the changes in zonal anatomy, age, and disease status may contribute to the diagnosis. However, different cut-off values are needed. Prospective larger scale studies are required to address this topic.

Conflict of Interest

The authors declare that they have no conflict of interest.

Authors' Contributions

Conceptualization, L.K.; methodology, L.K., Z.M.O., A.K.; formal analysis, L.K., Z.M.O. and M.S.; resources, L.K., Z.M.O., A.K. ; data curation, S.K, H.Ç; writing-original draft preparation, L.K.; writing-review and editing, L.K., Z.M.O., A.K., H.Ç., S.K., supervision, L.K., A.K., Z.M.O. All authors have read and agreed to the published version of the manuscript.

Ethics Approval

The study was conducted in accordance with the Declaration of Helsinki and approved by the Ethics Committee of Inönü University review boards, Malatya, Türkiye (protocol code 2021/162).

Informed Consent

Written informed consent was obtained.

Availability of Data and Materials

The datasets are not publicly available but are available from the corresponding author upon reasonable request.

ORCID ID

L. Karaca: 0000-0001-9150-3823
ZM. Özdemir: 0000-0003-1085-8978
A. Kahraman: 0000-0002-2147-1181
H. Çelik: 0000-0002-7180-4845
S. Kaya: 0000-0001-6936-7394

References

1) Jemal A, Siegel R, Xu J, Ward E. Cancer statistics, 2010. CA Cancer J Clin 2010; 60: 277-300.

2) Hara N, Okuizumi M, Koike H, Kawaguchi M, Bilim V. Dynamic contrast-enhanced magnetic resonance imaging (DCE-MRI) is a useful modality for the precise detection and staging of early prostate cancer. Prostate 2005; 62: 140-147.

3) Li X, Priest RA, Woodward WJ, Siddiqui F, Beer TM, Garzotto MG, Rooney WD, Springer CS. Cell membrane water exchange effects in prostate DCE-MRI. J Magn Reson 2012; 218: 77-85.

4) Fennessy FM, Fedorov A, Penzkofer T, Kim KW, Hirsch MS, Vangel MG, Masry P, Flood TA, Chang MC, Tempany CM, Mulkern RV, Gupta SN. Quantitative pharmacokinetic analysis of prostate cancer DCE-MRI at 3T: comparison of two arterial input functions on cancer detection with digitized whole mount histopathological validation. Magn Reson Imaging 2015; 33: 886-894.

5) Gao P, Shi C, Zhao L, Zhou Q, Luo L. Differential diagnosis of prostate cancer and noncancerous tissue in the peripheral zone and central gland using the quantitative parameters of DCE-MRI: A meta-analysis. Medicine (Baltimore) 2016; 95: e5715.

6) Turkbey B, Brown AM, Sankineni S, Wood BJ, Pinto PA, Choyke PL. Multiparametric prostate magnetic resonance imaging in the evaluation of prostate cancer. CA Cancer J Clin 2016; 66: 326-336.

7) Parra NA, Pollack A, Chinea FM, Abramowitz MC, Marples B, Munera F, Castillo R, Kryvenko ON, Punnen S, Stoyanova R. Automatic Detection and Quantitative DCE-MRI Scoring of Prostate Cancer Aggressiveness. Front Oncol 2017; 7: 259.

8) Chatterjee A, He D, Fan X, Wang S, Szasz T, Yousuf A, Pineda F, Antic T, Mathew M, Karczmar GS, Oto A. Performance of Ultrafast DCE-MRI for Diagnosis of Prostate Cancer. Acad Radiol 2018; 25: 349-358.

9) Heverhagen JT, von Tengg-Kobligk H, Baudendistel KT, Jia G, Polzer H, Henry H, Levine AL, Rosol TJ, Knopp MV. Benign prostate hyperplasia: evaluation of treatment response with DCE MRI. MAGMA 2004; 17: 5-11.

10) Somford DM, Futterer JJ, Hambrock T, Barentsz JO. Diffusion and perfusion MR imaging of the prostate. Magn Reson Imaging Clin N Am 2008; 16: 685-695.

11) Viswanath S, Bloch BN, Genega E, Rofsky N, Lenkinski R, Chappelow J, Toth R, Madabhushi A. A comprehensive segmentation, registration, and cancer detection scheme on 3 Tesla in vivo prostate DCE-MRI. Med Image Comput Comput Assist Interv 2008; 11: 662-669.

12) Lowry M, Zelhof B, Liney GP, Gibbs P, Pickles MD, Turnbull LW. Analysis of prostate DCE-MRI: comparison of fast exchange limit and fast exchange regimen pharmacokinetic models in the discrimination of malignant from normal tissue. Invest Radiol 2009; 44: 577-584.

13) Scherr MK, Seitz M, Muller-Lisse UG, Ingrisch M, Reiser MF, Muller-Lisse UL. MR-perfusion (MRP) and diffusion-weighted imaging (DWI) in prostate cancer: quantitative and model-based gadobenate dimeglumine MRP parameters in detection of prostate cancer. Eur J Radiol 2010; 76: 359-366.

14) Baccos A, Schiavina R, Zukerman Z, Busato F, Gaudiano C, Salizzoni E, Fiorentino M, Golfieri R, Martorana G. Accuracy of endorectal Magnetic Resonance Imaging (MRI) and Dynamic Contrast Enhanced-MRI (DCE-MRI) in the preoperative local staging of prostate cancer. Urologia 2012; 79: 116-122.

15) Michoux N, Simoni P, Tombal B, Peeters F, Machiels JP, Lecouvet F. Evaluation of DCE-MRI postprocessing techniques to assess metastatic bone marrow in patients with prostate cancer. Clin Imaging 2012; 36: 308-315.

16) Li X, Priest RA, Woodward WJ, Tagge IJ, Siddiqui F, Huang W, Rooney WD, Beer TM, Garzotto MG, Springer CS. Feasibility of shutter-speed DCE-MRI for improved prostate cancer detection. Magn Reson Med 2013; 69: 171-178.

17) Berman RM, Brown AM, Chang SD, Sankineni S, Kadakia M, Wood BJ, Pinto PA, Choyke PL, Turkbey B. DCE MRI of prostate cancer. Abdom Radiol 2016; 41: 844-853.

18) Fabijanska A. A novel approach for quantification of time-intensity curves in a DCE-MRI image series with an application to prostate cancer. Comput Biol Med 2016; 73: 119-130.

19) Hectors SJ, Besa C, Wagner M, Jajamovich GH, Haines GK, 3rd, Lewis S, Tewari A, Rastinehad A, Huang W, Taouli B. DCE-MRI of the prostate using shutter-speed vs. Tofts model for tumor characterization and assessment of aggressiveness. J Magn Reson Imaging 2017; 46: 837-849.

20) Al Salmi I, Menezes T, El-Khodary M, Monteiro S, Haider EA, Alabousi A. Prospective evaluation of the value of dynamic contrast enhanced (DCE) imaging for prostate cancer detection, with pathology correlation. Can J Urol 2020; 27: 10220-10227.

21) Onwuharine EN, Clark AJ. Comparison of double inversion recovery magnetic resonance imaging (DIR-MRI) and dynamic contrast enhanced magnetic resonance imaging (DCE-MRI) in detection of prostate cancer: A pilot study. Radiography 2020; 26: 234-239.

22) Abreu-Gomez J, Lim C, Cron GO, Krishna S, Sadoughi N, Schieda N. Pharmacokinetic modeling of dynamic contrast-enhanced (DCE)-MRI in PI-RADS category 3 peripheral zone lesions: preliminary study evaluating DCE-MRI as an imaging biomarker for detection of clinically significant prostate cancers. Abdom Radiol 2021; 46: 4370-4380.

23) Tofts PS, Brix G, Buckley DL, Evelhoch JL, Henderson E, Knopp MV, Larsson HB, Lee TY, Mayr NA, Parker GJ, Port RE, Taylor J, Weisskoff RM. Estimating kinetic parameters from dynamic contrast-enhanced T(1)-weighted MRI of a diffusable tracer: standardized quantities and symbols. J Magn Reson Imaging 1999; 10: 223-232.

24) Parra NA, Lu H, Li Q, Stoyanova R, Pollack A, Punnen S, Choi J, Abdalah M, Lopez C, Gage K, Park JY, Kosj Y, Pow-Sang JM, Gillies RJ, Balagurunathan Y. Predicting clinically significant prostate cancer using DCE-MRI habitat descriptors. Oncotarget 2018; 9: 37125-37136.

25) Taghipour M, Ziaei A, Alessandrino F, Hassanzadeh E, Harisinghani M, Vangel M, Tempany CM, Fennessy FM. Investigating the role of DCE-MRI, over T2 and DWI, in accurate PI-RADS v2 assessment of clinically significant peripheral zone prostate lesions as defined at radical prostatectomy. Abdom Radiol 2019; 44: 1520-1527.

26) Afshari Mirak S, Mohammadian Bajgiran A, Sung K, Asvadi NH, Markovic D, Felker ER, Lu D, Sisk A, Reiter RE, Raman SS. Dynamic contrast-enhanced (DCE) MR imaging: the role of qualitative and quantitative parameters for evaluating prostate tumors stratified by Gleason score and PI-RADS v2. Abdom Radiol 2020; 45: 2225-2234.

27) Uysal A, Karaosmanoglu AD, Karcaaltincaba M, Akata D, Akdogan B, Baydar DE, Ozmen MN. Prostatitis, the Great Mimicker of Prostate Cancer: Can We Differentiate Them Quantitatively

With Multiparametric MRI? AJR Am J Roentgenol 2020; 215: 1104-1112.

28) van Niekerk CG, Witjes JA, Barentsz JO, van der Laak JA, Hulsbergen-van de Kaa CA. Microvascularity in transition zone prostate tumors resembles normal prostatic tissue. Prostate 2013; 73: 467-475.

29) Cannarella R, Condorelli RA, Barbagallo F, La Vignera S, Calogero AE. Endocrinology of the Aging Prostate: Current Concepts. Front Endocrinol 2021; 12: 554078.

30) Padhani AR, Gapinski CJ, Macvicar DA, Parker GJ, Suckling J, Revell PB, Leach MO, Dearnaley DP, Husband JE. Dynamic contrast-enhanced MRI of prostate cancer: correlation with morphology and tumour stage, histological grade and PSA. Clin Radiol 2000; 55: 99-109.

31) Ma XZ, Lv K, Sheng JL, Yu YX, Pang PP, Xu MS, Wang SW. Application evaluation of DCE-MRI combined with quantitative analysis of DWI for the diagnosis of prostate cancer. Oncol Lett 2019; 17: 3077-3084.

32) Kozlowski P, Chang SD, Jones EC, Berean KW, Chen H, Goldenberg SL. Combined diffusion-weighted and dynamic contrast-enhanced MRI for prostate cancer diagnosis--correlation with biopsy and histopathology. J Magn Reson Imaging 2006; 24: 108-113.

33) Cai W, Li F, Wang J, Du H, Wang X, Zhang J, Fang J, Jiang X. A comparison of arterial spin labeling perfusion MRI and DCE-MRI in human prostate cancer. NMR Biomed 2014; 27: 817-825.

34) van Dorsten FA, van der Graaf M, Engelbrecht MR, van Leenders GJ, Verhofstad A, Rijpkema M, de la Rosette JJ, Barentsz JO, Heerschap A. Combined quantitative dynamic contrast-enhanced MR imaging and (1)H MR spectroscopic imaging of human prostate cancer. J Magn Reson Imaging 2004; 20: 279-287.